European Journal of Cell Biology 102 (2023) 151302

Contents lists available at ScienceDirect

European Journal of Cell Biology

journal homepage: www.elsevier.com/locate/ejcb

GSK-3 inhibition reverts mesenchymal transition in primary human corneal endothelial cells

Eleonora Maurizi [a,*], Alessia Merra [a,b], Claudio Macaluso [c], Davide Schiroli [d,*], Graziella Pellegrini [a,b]

[a] Centre for Regenerative Medicine, University of Modena and Reggio Emilia, Modena, Italy
[b] Holostem Terapie Avanzate S.r.l., Modena, Italy
[c] Dentistry center, University of Parma, Parma, Italy
[d] Transfusion Medicine Unit, USL-IRCCS, Reggio Emilia, Italy

ARTICLE INFO

Keywords:
Human corneal endothelial cells
Endothelial mesenchymal transition
CHIR99021
Proliferation
Differentiation

ABSTRACT

Human corneal endothelial cells are organized in a tight mosaic of hexagonal cells and serve a critical function in maintaining corneal hydration and clear vision. Regeneration of the corneal endothelial tissue is hampered by its poor proliferative capacity, which is partially retrieved in vitro, albeit only for a limited number of passages before the cells undergo mesenchymal transition (EnMT). Although different culture conditions have been proposed in order to delay this process and prolong the number of cell passages, EnMT has still not been fully understood and successfully counteracted. In this perspective, we identified herein a single GSK-3 inhibitor, CHIR99021, able to revert and avoid EnMT in primary human corneal endothelial cells (HCEnCs) from old donors until late passages in vitro (P8), as shown from cell morphology analysis (circularity). In accordance, CHIR99021 reduced expression of α-SMA, an EnMT marker, while restored endothelial markers such as ZO-1, Na^+/K^+ ATPase and N-cadherin, without increasing cell proliferation. A further analysis on RNA expression confirmed that CHIR99021 induced downregulation of EnMT markers (α-SMA and CD44), upregulation of the proliferation repressor p21 and revealed novel insights into the β-catenin and TGFβ pathways intersections in HCEnCs. The use of CHIR99021 sheds light on the mechanisms involved in EnMT, providing a substantial advantage in maintaining primary HCEnCs in culture until late passages, while preserving the correct morphology and phenotype. Altogether, these results bring crucial advancements towards the improvement of the corneal endothelial cells based therapy.

1. Introduction

The innermost layer of the cornea, the corneal endothelium (CE), efficiently transports solutes from and to the aqueous humor, thus maintaining corneal transparency and function. Corneal endothelial cells (CEnCs) are poorly mitotic in vivo (Joyce, 2005), as a consequence of the sealed tight cell-cell junctions and the presence of proliferative inhibitors in the aqueous humor (Lee and Kay, 2008; Paull and Whikehart, 2005). Cell migration and enlargement (Joyce, 2005; Van den Bogerd et al., 2018) are the mechanisms that counteract a constant decrease in cell density (0.6% every year) (Ali et al., 2016; Waring et al., 1982); nevertheless exogenous factors, such as surgical interventions, infections or physical trauma, and corneal diseases may irreversibly damage the CE, thus impairing this delicate equilibrium. In this case, an altered CE becomes unable to play its function (Van den Bogerd et al., 2018), leading to corneal opacification and, in the last instance, to blindness. To date, transplantation is the only accepted treatment to cure irreversibly damaged corneas, for which CE dysfunction represents the most frequent indication (Català et al., 2021). Although quite diffused and generally safe, corneal grafts are not equally accessible worldwide and still present a relevant failure rate (Català et al., 2021).

Since CEnCs are able to acquire, albeit in a limited manner, a proliferative capacity in culture, researchers are willing to promote CE regeneration directly in vivo or in vitro (Català et al., 2021; Maurizi et al., 2022a), prior to transplantation.

In the first-in-human clinical trial, Kinoshita's group successfully transplanted human (H)CEnCs obtained from young donors and expanded for a maximum of three passages in culture (Kinoshita et al.,

* Corresponding authors.
E-mail addresses: eleonora.maurizi@unimore.it (E. Maurizi), davide.schiroli@ausl.re.it (D. Schiroli).

https://doi.org/10.1016/j.ejcb.2023.151302
Received 15 December 2022; Received in revised form 18 February 2023; Accepted 5 March 2023
Available online 7 March 2023

2018). Nevertheless, several improvements are still necessary since HCEnCs easily alter their morphology and function in vitro (Frausto et al., 2020). This impairment, which is exacerbated in cells from older donors, drastically increases with passages and is mainly a consequence of mesenchymal transformation (endothelial to mesenchymal transition, EnMT) (Roy et al., 2015), a cellular process occurring also in cancer cells, and during normal expansion of several stem cells (Lambert and Weinberg, 2021). In line with this observation, EnMT might represent a physiological and reversible process that naturally underlies HCEnCs migration and proliferation. However, if EnMT is dysregulated, for instance during in vitro expansion when HCEnCs are induced to leave their quiescence (G0/G1) and become proliferative (G2), it may lead to an irreversible mesenchymal transformation (Roy et al., 2015). EnMT transformed HCEnCs (positive for specific markers such as α-SMA), arise not only after passaging (Maurizi et al., 2022b), but also consequently to the cell junctions disruption following EDTA treatment (Zhu et al., 2012), as well as upon growth factors stimulation (Gu et al., 1996; Leclerc et al., 2018; Lee et al., 2012; Maurizi et al., 2020; Zhu et al., 2012). It has been largely documented that epithelial and fibroblast growth factors (EGF and FGF, respectively) are able to promote cellular proliferation while preserving the cellular phenotype (Joyce, 2004; Li et al., 2007; Peh et al., 2011), but only for few passages (Gu et al., 1996; Leclerc et al., 2018; Lee et al., 2018, 2012; Maurizi et al., 2020; Zhu et al., 2012), while transforming growth factor (TGFβ) induces EnMT upon certain conditions (Leclerc et al., 2018). HCEnCs undergoing a mesenchymal transformation present with an altered cellular functionality, mainly caused by the loss of cellular structure (in terms of polarity, motility, extracellular matrix production, cytoskeleton modifications and loss of cellular contacts) (Roy et al., 2015). As a consequence, EnMT transformed HCEnCs are not suitable for developing a cell therapy as they are not able to reproduce an intact and functional endothelium, but they can induce tissue fibrosis (Lee et al., 2018). Although the maximum number of passages that HCEnCs reach in culture depends primarily on donor characteristics, EnMT represents one of the main hurdles limiting in vitro expansion. Aiming at increasing the maximum number of passages, researchers have investigated some alternative culture media conditions to promote proliferation and stem at the same time EnMT undesired effects (Català et al., 2021; Okumura et al., 2015, 2013; Peh et al., 2015). In particular TGFβ (Okumura et al., 2013) and ROCK pathway inhibition (Okumura et al., 2012) and, more recently, a dual media approach (the first during the proliferative state and the second of maintenance) (Bartakova et al., 2018; Parekh et al., 2019, 2021; Peh et al., 2015) have found a large consensus (Català et al., 2021; Frausto et al., 2020) as valid solutions to preserve HCEnCs phenotype. Nevertheless, no key mechanisms able to revert the EnMT and possible approaches to reach this aim have been successfully proposed. Some hints support the hypothesis that the β-catenin pathway might be a reasonable target: i) The Wnt/β-catenin pathway is finely regulated in other cell types to switch from a proliferative to a differentiate state (Gao et al., 2021; Nusse et al.). ii) Dysregulation of this pathway is an important player in mesenchymal transformation (Distler et al., 2019; Zhang et al., 2016). iii) β-catenin involvement was previously linked to this delicate balance from us and other groups in HCEnCs (Hirata-Tominaga et al., 2013; Lee and Heur, 2015; Maurizi et al., 2020; Zhu et al., 2012). Moreover, we recently proved that β-catenin pathway is finely tuned when CEnCs are dissected and expanded in vitro (Maurizi et al., 2020). This pathway resulted fundamental to maintain proliferation, while its activation through a small molecule CHIR99021 was not able to increase cellular proliferation. We also measured the α-SMA positive cells at low passage in rabbit primary CEnCs and we found a small but not significant decrease of this parameter. CHIR99021 has been largely used to induce cellular differentiation (Laco et al., 2018; Lam et al., 2014; Leach et al., 2015), acting on the β-catenin stability. In corneal endothelium it promotes the direct transformation of corneal stroma precursors cells to corneal endothelial cells (Hatou et al., 2013) and recently Wang and collaborators showed that it was able to counteract the TGFβ1 induced cell modification, in particular α-SMA overexpression, in a cell line of corneal endothelium (Wang et al., 2022b). Starting from these pieces of evidence, we demonstrate here the CHIR99021 capability to both avoid and revert EnMT in primary HCEnC from old donor corneas during in vitro expansion, up to high passages (P8).

2. Materials and methods

2.1. Primary HCEnCs culture

Human corneal tissues were preserved in Eusol at 4 °C and used within 15 days from the donor's death; a list of details for each cornea used and relative experiments is shown in Supplementary Table 1. Except from one donor who was 26 and another who was 51 years old, the majority ranged from 63 to 81 years old. HCEnCs were isolated through Descemet's stripping and digestion with 1.5 mg/mL Collagenase A (Roche) for 3 h (h) at 37 °C. After 5 min (min) in TrypLE (Thermo Fisher Scientific) at 37 °C, HCEnCs were pelleted at 1200 rpm (240 rcf) for 3 min and plated on FNC Coating mix (AthenaES) treated wells.

HCEnCs were cultured at 37 °C in 5% CO_2, changing the growth medium every other day. The growth medium is composed of OptiMEM-I (Thermo Fisher Scientific), 8% HyClone fetal bovine serum (FBS; Fisher Scientific), 5 ng/mL epidermal growth factor (EGF; Thermo Fisher Scientific), 20 μg/mL ascorbic acid (Sigma-Aldrich), 200 mg/L calcium chloride (Sigma-Aldrich), 0.08% chondroitin sulphate (C4384, Sigma-Aldrich), and penicillin/streptomycin (Euroclone). Upon confluency, HCEnCs were rinsed in DPBS and passaged at a ratio of 1:2 or 1:3 with TrypLE (Thermo Fisher Scientific) for 10–15 min at 37 °C in 5% CO_2. Sub-confluent cultures were harvested 24 h after plating.

CHIR99021 (SML1046, Sigma-Aldrich, concentration range of 0.1–10 μM) and TGFβ inhibitor (TGFβI, SB431542, Sigma-Aldrich, 1 μM) were added to the culture media and replaced at any medium change. The control condition refers to cells treated with DMSO only and showed no significant morphological, proliferation and expression differences with untreated HCEnCs.

2.2. Immunofluorescence

Immunofluorescence staining was performed on primary cultured HCEnCs after fixation in 3% PFA, 15 min at room temperature (RT) or Methanol for β-catenin, 10 min at − 20 °C. Triton X-100 (Bio-Rad) used at 1% for 10 min at RT allowed cell permeabilization and a solution of bovine serum albumin (BSA; Sigma-Aldrich) 2%, FBS 2%, Triton X-100 at 0.01% in PBS was used for 30 min at 37 °C to block the non-specific binding sites. Primary and secondary antibodies were incubated for 1 h at 37 °C while nuclei were counterstained with DAPI (Roche) at RT for 5 min before mounting the glass coverslips using DAKO mounting medium (Agilent). Primary antibodies used herein are listed in Supplementary Table 2 while secondary antibodies used are: Alexa Fluor 488 anti-rabbit, 1:2000, and Alexa Fluor 568 anti-mouse, 1:1000 (Thermo Fisher Scientific). Images were obtained with a confocal microscope (LSM900 Airyscan—Carl Zeiss).

Quantification of α-SMA staining was obtained by counting the number of positive cells (primary antibody signal), relative to the total number of cells in that field (DAPI staining). The values obtained from cells of different donors were expressed in percentage with standard deviation (three fields for each replicate were collected).

CellEvent® Caspase 3/7 Green (Thermo Fisher, UK) was used to evaluate cell apoptosis, following the manufacturer's instructions. As a positive control for this assay, HCEnCs were treated with 10 mM H_2O_2 for 2 h.

2.3. Cell circularity

Cell circularity was determined using ImageJ software: morphometric values of the perimeter and area of cells were obtained from

phase contrast images of the culture by manually outlining each cell borders, as shown in previously published papers (Peh et al., 2015). An average of 50 cells for each condition were analysed, from three different donors each (n = 3).

A perfect circle has a circularity value of 1: polygonal HCEnCs have a value closer to 1 if compared with HCEnCs with an elongated fibroblastic morphology, which circularity is closer to zero.

2.4. Cell cycle analysis by FACS

The cell cycle was studied by staining sub-confluent cultures of HCEnCs with Propidium Iodide (PI; Sigma-Aldrich). HCEnCs suspension from cell culture was washed with DPBS and incubated for 1 h at 4 °C in the dark with 250 μL of a PBS solution composed by PI 50 μg/mL, Triton X-100 (Bio-Rad, USA) at 0.1%. Cells were then analysed using BD FACS Canto II (BD BIOSCIENCES; San Jose, CA USA). For each sample, 20,000 events were considered for the analysis to ensure statistical relevance and results were analysed with a ModFit 3.0 software.

2.5. RT-PCR

HCEnCs RNA was extracted by RNeasy plus Micro Kit (Qiagen), quantified with Nanodrop 100 (Thermo Fisher Scientific) and reverse transcribed by the High Capacity cDNA Reverse Transcription Kit (Thermo Fisher Scientific).

7900HT Fast Real-Time PCR System (Thermo Fisher Scientific) was used for RT-PCR assays, using the TaqMan Real Time PCR Assays probes and primers for SyBr Green listed in Supplementary Table 3 and 4.

GAPDH was used as housekeeping control and ΔCt and ΔΔCt calculations were performed to evaluate effective RNA expression. Each gene was evaluated in cells deriving from three different donors for each condition, in two donors for the TGFβI analysis.

2.6. Western blot

Western blot analysis was carried out on HCEnCs collected by trypsinization. HCEnCs proteins were extracted using RIPA lysis buffer (R0278, Sigma), supplemented with protease and phosphatase inhibitors (97786, 78420, Thermo Fisher) and quantified by Bradford assay (5000205—Bio Rad). Equivalent amount of proteins were diluted in LDS Sample Buffer 4X and Sample reducing agent 10X (Thermo Fisher), boiled for 10 min at 90 °C and loaded (100 V for 30 min and at 150 V for 1 h) in a 4–12% NuPAGE Bis-Tris Gels (Thermo Fisher). HCEnCs proteins were resolved and then transferred to a nitrocellulose membrane (Bio Rad) for 2 h at 100 V at 4 °C, which was blocked afterwards for 5 min at room temperature using Every Blot blocking buffer (Bio Rad). The membranes were then probed with primary antibodies diluted in blocking solution: α-SMA (A5228, Sigma) 1:1000 and Vinculin (V4505, Sigma) at 1:10000, incubated overnight at 4 °C. Horseradish peroxidase-coupled secondary antibodies (ab6789, Abcam), used at 1:10000 dilution for 1 h at room temperature, and a chemiluminescent substrate (SuperSignal West Pico, 34080, Thermo Fisher) allowed visualization of the protein bands at the correct molecular weight through Chemi-Doc (Bio Rad). Vinculin has been used as housekeeping as not variating in HCEnCs at confluency (Parekh et al., 2017).

2.7. Statistical analysis

Microsoft Excel 2010 and GraphPad Prism 5 software were used for data and statistical analysis. Values were represented as mean ± standard deviation (SD). Statistical comparison was done using two-tailed Student's t-test, while gene expression data were compared with a Ratio Paired t-test. Significance was set at $p < 0.05$ and the number of replicates are indicated in each experiment.

3. Results

3.1. CHIR99021 (CHIR) regulates EnMT in primary cultures of HCEnCs

Primary HCEnCs were treated with CHIR99021 at different concentrations (1–3–10 μM) to evaluate its dose related effect upon EnMT (Fig. 1).

A clear variation of HCEnCs morphology was initially observed (Fig. 1 A): when CHIR99021 at 1–3 μM was added to the culture media, HCEnCs at passage 1 (P1) appeared as more polygonal if compared to the untreated control. An elongated morphology was observed instead whenever HCEnCs were treated with CHIR99021 at 10 μM. The immunocytochemistry analysis showed a reduced expression of α-SMA, marker of EnMT, in cells treated with CHIR99021 at 1–3 μM if compared to the control. HCEnCs positively stained for the α-SMA marker showed an elongated morphology if compared with HCEnCs that did not express α-SMA. CHIR used at 10 μM accelerated the process of EnMT, as observed from α-SMA expression that was increased in every cell (Fig. 1B). Quantification of the percentage of HCEnCs expressing α-SMA in immunofluorescence images shown in Fig. 1B demonstrates that the most effective CHIR99021 concentration, able to significantly reduce α-SMA expression to 9.2 ± 2.1% from 40.2 ± 5.2% of the control ($p = 0.0046$), was 1 μM (Fig. 1 C).

The maintenance of a hexagonal shape is a characteristic feature of HCEnCs and is fundamental for HCEnCs to exert their biological function (Bourne, 2003; Wörner et al., 2011). For this reason, a morphological study on cell morphology from Fig. 1 A allowed evaluating the variation of HCEnCs circularity between the conditions under investigation (Fig. 1D). HCEnCs treated with 1 μM CHIR99021 showed an average circularity value of 0.77, which is the closest to 1 (value of a perfect circle), if compared with the control (0.46), the 3 μM (0.69) and the 10 μM (0.25) CHIR99021 treated cells. CHIR99021 used at 1 μM was therefore chosen for all the subsequent experiments and will be indicated from now onwards as CHIR. As known from the literature, CHIR inhibits GSK-3β and thus stabilises intracellular β-catenin, as confirmed here in immunofluorescence analysis of HCEnCs at P4 (Fig. 1E). β-catenin positive nuclei were quantified, resulting in an increase to 30.4 ± 6.5% in CHIR treated cells from a 11.8 ± 0.44% of the control (Figure1F).

CHIR99021 at 1 μM demonstrated here its capacity to reduce the process of EnMT in primary HCEnCs by restoring cell morphology and decreasing the expression of α-SMA marker. These results are crucial to counteract the EnMT process that hampers the opportunity for these cells to be amplified in culture and thus to be used for further studies or for clinical application.

3.2. CHIR reverses the mesenchymal phenotype in primary cultures of HCEnCs

Primary HCEnCs, already presenting an elongated morphology (P3), were treated with CHIR for several subsequent passages in culture: CHIR demonstrated capable of reverting the mesenchymal phenotype at any passage (Fig. 2).

A schematic diagram illustrates the experimental design for treating the spindle-shaped HCEnCs with CHIR from P3 to P8 (Fig. 2 A).

The morphological reversion of HCEnCs mesenchymal phenotype was observed in CHIR treated cells as compared to the control, at each passage in culture until P8 (Fig. 2B). Cell circularity quantified the morphological transformation: a significant difference in cell circularity between CHIR and control samples was detected from the first CHIR application (P3, $p = 0.004$) and maintained until P8 ($p < 0.0001$) (Fig. 2 C).

CHIR treated samples presented a consistent decrease in α-SMA protein expression either at low or high passages (a representative image is shown for P5 in Fig. 2D). Quantification of the immunofluorescence results showed that α-SMA expression was reduced in CHIR treated

HCEnCs at P2, P5 and P7 to 7.6 ± 4.4%, 14.1 ± 1.9% and 16.3 ± 1.8% from its initial value of 31.3 ± 3.2%, 33.4 ± 4.5%, 37.2 ± 1.7%, respectively (Fig. 2E). A decrease in α-SMA protein expression was furtherly observed in HCEnCs treated with CHIR at P9 by western blot analysis, when compared with its relative control (Supplementary Figure 1).

The results obtained highlight that primary HCEnCs that underwent EnMT, if stimulated with CHIR, can reacquire their characteristic polygonal morphology and lose the α-SMA marker for several subsequent passages in culture.

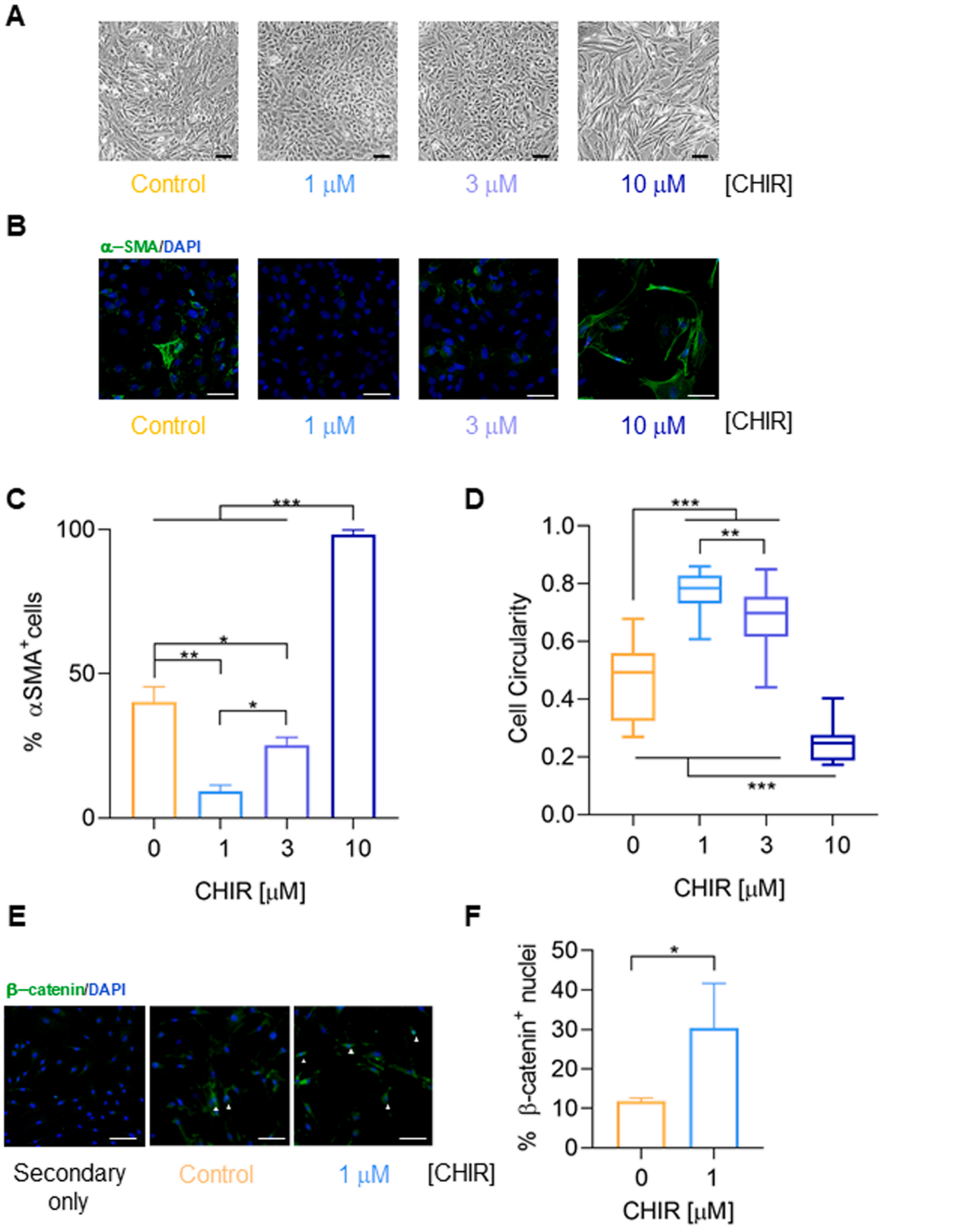

(caption on next page)

Fig. 1. CHIR99021 titration in primary cultures of human corneal endothelial cells (HCEnCs). A) Representative phase-contrast images of primary HCEnCs culture at passage 1 (P1), showing the morphology differences between cells treated with CHIR99021 at different concentrations (1–3 - 10 μM) and control. Scale bar 100 μm. B) Representative immunofluorescence microscopy images of HCEnCs at P1, showing expression of the α-SMA (green) EnMT marker on CHIR99021 treated and untreated HCEnCs. DAPI (blue) counterstains nuclei. Scale bar 50 μm. C) Quantification of the percentage of HCEnCs expressing α-SMA protein in samples treated with CHIR99021 at different concentrations (1–3 - 10 μM) were compared with their relative untreated control, as seen in Fig. 1B. D) Box plot comparing cell circularity values between HCEnCs treated with CHIR99021 at different concentrations (1–3 - 10 μM) and their relative untreated control (n = 3). E) Representative immunofluorescence microscopy images of HCEnCs at P4 showing expression of the β-catenin (green) on HCEnCs treated and untreated with CHIR99021 at 1 μM (CHIR). DAPI (blue) counterstains nuclei, white arrows indicate where β-catenin shows a nuclear signal. Scale bar 50 μm. F) Quantification of the percentage of HCEnCs expressing nuclear β-catenin protein in samples treated with CHIR, as compared with their relative untreated control, as seen in Fig. 1E. Quantitative data are expressed as values ± SD. Statistical significance was assessed using a Student t-test and set at $p < 0.05$. p values are indicated as following: ns (not significative) when $p > 0.05$, * when $p < 0.05$, * * when $p < 0.01$, * ** when $p < 0.001$. (For interpretation of the references to colour in this figure legend, the reader is referred to the web version of this article.)

3.3. CHIR helps maintaining the correct expression and localization of HCEnCs markers

A deeper analysis of CHIR effects, protein expression and localization, as well as of multiple culture conditions was conducted to try elucidating its mechanism on HCEnCs (Fig. 3).

A comparison between CHIR treated and untreated HCEnCs showed that several corneal endothelial markers such as Na^+/K^+ ATPase, ZO-1, β-catenin and N-cadherin were expressed correctly only in the CHIR treated HCEnCs, while they were absent and/or delocalised in the untreated control (Fig. 3A). A caspase 3/7 assay was carried out in parallel to exclude the possibility of apoptosis events due to CHIR treatment.

Fig. 3 B represents a comparison between CHIR previously treated and untreated HCEnCs the day after plating, before adding CHIR to the culture media (representative images obtained at P6). At any passage, HCEnCs appeared with a similar spindle shaped morphology at subconfluency, which reverted to a polygonal morphology once at confluence if CHIR was added, while it remained elongated in the untreated control.

To determine if the CHIR effect could be exerted even at later passages, HCEnCs culture was further divided by adding two conditions at P6: in one CHIR was removed from the previously CHIR treated cells; while in the other CHIR was added to the cells that had not been treated before (Fig. 3C, P6 b). Whenever at confluence, the samples where CHIR was later removed lost the polygonal morphology, while the control samples where CHIR was added only at P6 reacquired a polygonal morphology (a schematic is shown in Fig. 3D). This tendency was confirmed by evaluation of cell circularity (Fig. 3E): CHIR addition was able to revert the phenotype even at late passages, with HCEnCs presenting a circularity of 0.52, significantly different from the circularity of HCEnCs deprived of CHIR, equal to 0.26 ($p < 0.0001$).

Taken together, these results indicate how CHIR addition promotes the correct expression and localization of corneal endothelial characterizing proteins. At any passage, either in CHIR or control samples, cells cross an intermediate phase at subconfluence when they show an elongated morphology. The restoration of polygonal morphology can be induced by adding CHIR even at late passages in culture while it is abolished when, upon cell passaging, CHIR is removed.

3.4. CHIR allows maintaining a polygonal phenotype in primary cultures of HCEnCs

Primary HCEnCs that still retained a polygonal morphology (P2), were treated with CHIR for several subsequent passages to evaluate the CHIR capacity to maintain the correct morphology and prevent the EnMT process (Fig. 4).

A scheme of the experimental design is shown in Fig. 4 A. CHIR was added to the culture media at any passage and compared with its relative untreated HCEnCs control: morphological differences started becoming evident at P3 and the discrepancy between the two conditions raised up as the passages increased (Fig. 4B).

Quantification of cell circularity revealed a significant difference between CHIR treated and untreated control (Fig. 4 C), starting from P5 ($p < 0.0001$) and increasing progressively, until P8 ($p < 0.0001$).

These data reveal how CHIR can prevent the loss of polygonal phenotype in primary HCEnCs for multiple passages in culture. This mechanism could be exploited to maintain HCEnCs in culture for a longer period of time, while they preserve the correct morphology.

3.5. CHIR reduces cell proliferation rate in primary cultures of HCEnCs

Cell proliferation upon CHIR treatment was studied with multiple techniques (Fig. 5).

For the sample groups treated before or after acquiring an elongated morphology, the cells were counted upon confluency at any passage and compared between the CHIR treated and control HCEnCs (Fig. 5 A). The number of CHIR treated HCEnCs was constantly lower with respect to their relative untreated control, similarly in both sample groups. The following experiments on cell proliferation were carried out on the group sample that started treatment before changing morphology.

Immunofluorescence analysis on HCEnCs at P5 revealed an equal or lower amount of cells expressing the ki67 proliferation marker in CHIR treated cells, as evaluated in cells isolated from three different donors (Fig. 5B and C).

A reduction in cell proliferation rate is confirmed by FACS analysis on sub-confluent HCEnCs cultures at high passages (P5 - P7 - P8), whenever the two conditions (CHIR-control) demonstrated a significant morphological difference between them at the previous passage upon confluency. In all the three passages analysed, CHIR enhanced the percentage of cells in G0/G1 phase of the cell cycle and concomitantly reduced the percentage of cells at G2/M (Fig. 5D).

The data obtained demonstrate that CHIR addition in primary HCEnCs cultures inhibits the cell proliferation rate, as evaluated with different assays.

3.6. CHIR effects on gene expression in primary cultures of HCEnCs

A set of selected genes were analysed at RNA level to get novel insights into the mechanism of CHIR effect on preserving HCEnCs morphology and protein expression (Fig. 6).

At low passages, none of the selected genes showed any difference between the CHIR treated and untreated HCEnCs but we could appreciate a significant up- or down-regulation at high passages (P6-P7) for the following genes.

At high passages, genes related to HCEnCs cell cycle such as p21 and p27 have been investigated: CHIR stimulation induced an increased expression of p27 ($p = 0.06$) and p21 ($p = 0.02$), the latter resulting significant if compared with untreated cells (Fig. 6 A and 6B).

EnMT marker genes were found here significantly downregulated at RNA level upon CHIR treatment: α-SMA ($p = 0.03$) and CD44 ($p = 0.04$). This data is in accordance with the CHIR induced EnMT reduction, supported by a concomitant maintenance of hexagonal cell morphology and a decreased α-SMA protein expression, as shown above.

Surprisingly COL1A1, an important mediator of tissue wound healing (Mathew-Steiner et al., 2021), resulted upregulated at high passages following CHIR induced β-catenin stabilization ($p = 0.01$).

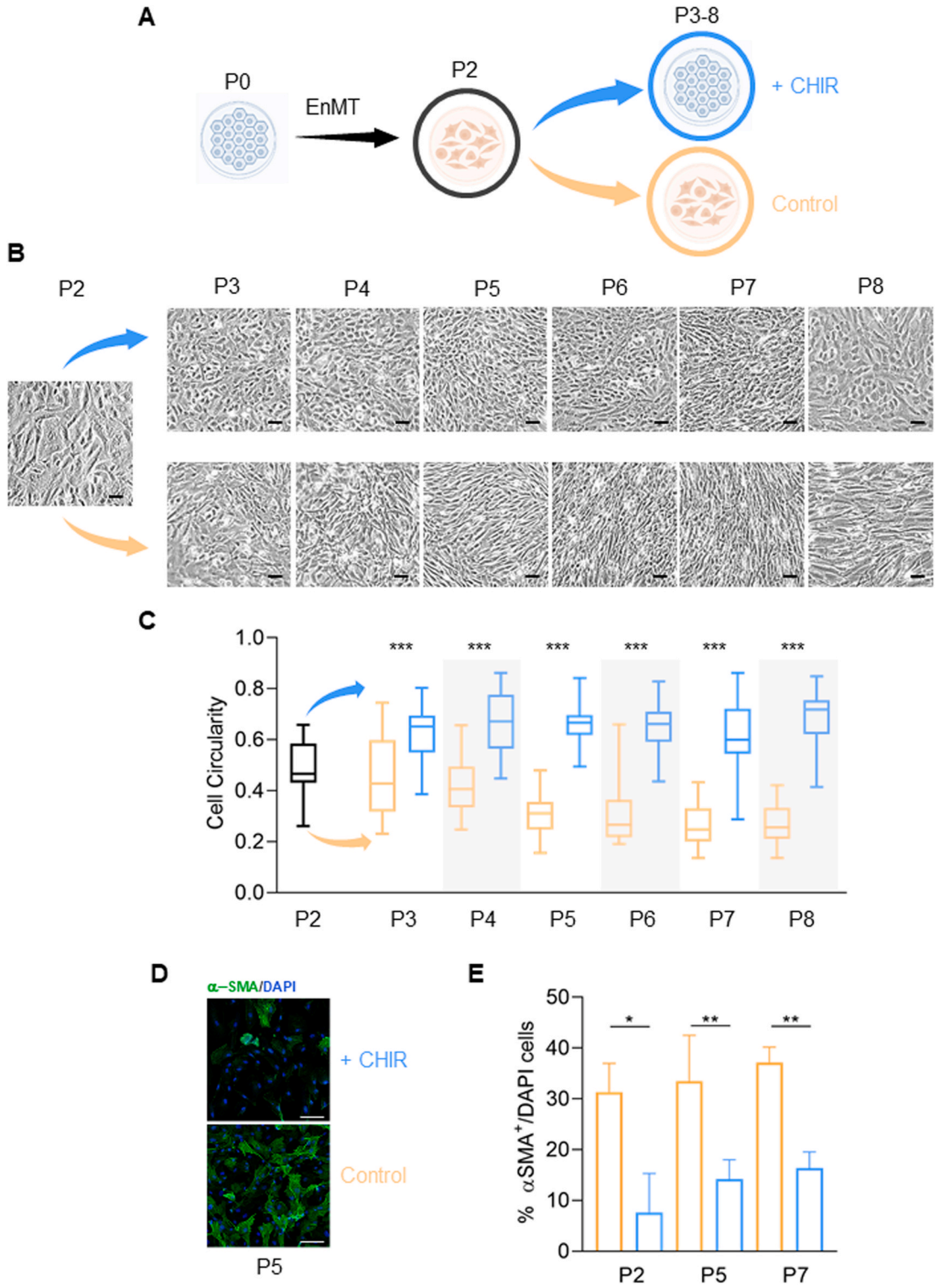

Fig. 2. CHIR reverses the mesenchymal phenotype in primary cultures of HCEnCs. A) Schematic representation of the experimental plan for CHIR addition to HCEnCs culture, after EnMT. Image created with Biorender.com B) Representative phase-contrast images of primary HCEnCs treated with 1 μM CHIR at progressive passages (P3 to P8) following EnMT, showing the morphological differences with the untreated HCEnCs (n = 3). Scale bar 100 μm. C) Box plot comparing cell circularity values between HCEnCs treated with CHIR and their relative untreated control (n = 3) at subsequent passages in culture. Cell circularity is expressed as values ± SD. D) Representative immunofluorescence microscopy images of HCEnCs at P5, showing expression of the α-SMA (green) EnMT marker on CHIR treated HCEnCs and their relative untreated control. DAPI (blue) counterstains nuclei. Scale bar 50 μm. E) Quantification of the percentage of HCEnCs expressing α-SMA protein (± SD) in samples treated with CHIR, compared with their relative untreated control, as seen in Fig. 2D. Statistical significance was assessed using a Student t-test and set at $p < 0.05$. p values are indicated as following: ns (not significative) when $p > 0.05$, * when $p < 0.05$, * * when $p < 0.01$, * ** when $p < 0.001$. (For interpretation of the references to colour in this figure legend, the reader is referred to the web version of this article.)

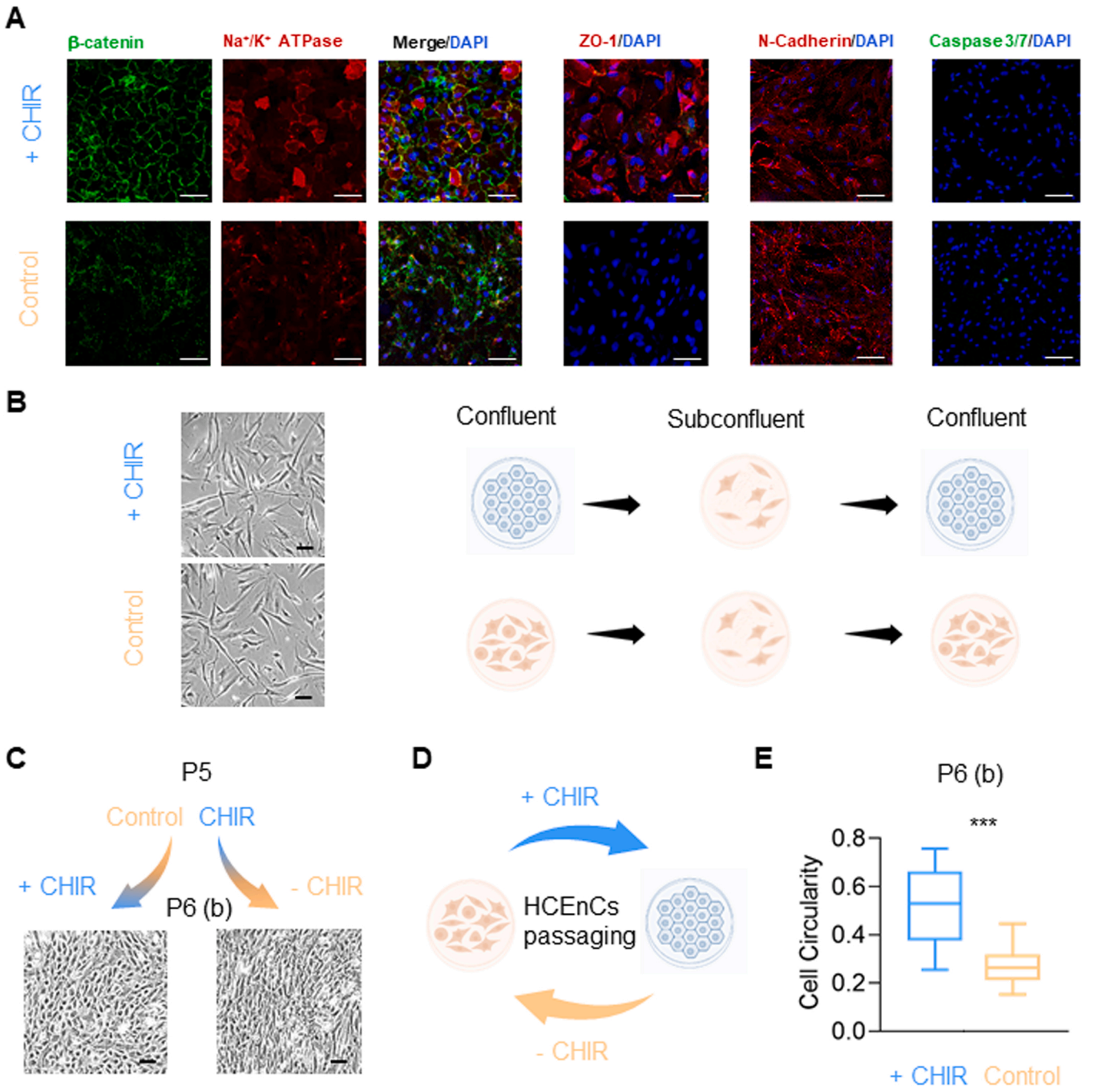

Fig. 3. CHIR restores corneal endothelial protein expression and morphology at later stages A) Representative immunofluorescence microscopy images showing expression of typical HCEnCs markers such as β-catenin (green, P7), Na^{+}/K^{+} ATPase (red, P7), ZO-1 (red, P5), N-cadherin (red, P4) and Caspase 3/7 (green, P5) on CHIR treated HCEnCs and their relative untreated control. DAPI (blue) counterstains nuclei. Scale bar 50 μm, for Caspase 3/7 only scale bar 100 μm. B) Representative phase-contrast images of sub-confluent HCEnCs the day after plating, before being treated with CHIR (P6), showing no morphological differences with the untreated HCEnCs. Scale bar 100 μm. A simplified scheme is shown on the right, done in Biorender.com. C) Representative phase-contrast images of HCEnCs untreated at P5 and treated with CHIR at P6, in parallel to HCEnCs treated with CHIR at P5, becoming untreated at P6. CHIR demonstrates to exert its effect also at a later stage, which is reversible upon passages. Scale bar 100 μm. D) Schematic representation of the HCEnCs morphological change upon passaging when treated with CHIR, done in Biorender.com. E) Box plot comparing cell circularity values between HCEnCs treated with CHIR and their relative untreated control from Fig. 3C. Cell circularity is expressed as values ± SD. Statistical significance was assessed using a Student t-test and set at $p < 0.05$. p values are indicated as following: ns (not significative) when $p > 0.05$, * when $p < 0.05$, * * when $p < 0.01$, * ** when $p < 0.001$. (For interpretation of the references to colour in this figure legend, the reader is referred to the web version of this article.)

Cdc42, a marker of the non-canonical Wnt pathway regulating HCEnCs migration (Lee and Heur, 2015), and Pitx2, a protein involved in the development of the cornea (Gage et al., 2014), were significantly upregulated in CHIR treated cells ($p = 0.01$ and $p = 0.03$, respectively).

Additional genes such as SOX2, involved in wound healing in CE (Chang et al., 2018), and Zeb1, found to mediate fibrosis in CE (Lee et al., 2020), were assessed herein and compared between CHIR treated and untreated cells but showed no significant differences and low levels of expression either at low or high passages (data not shown).

Expression analysis of selected genes confirmed an increased

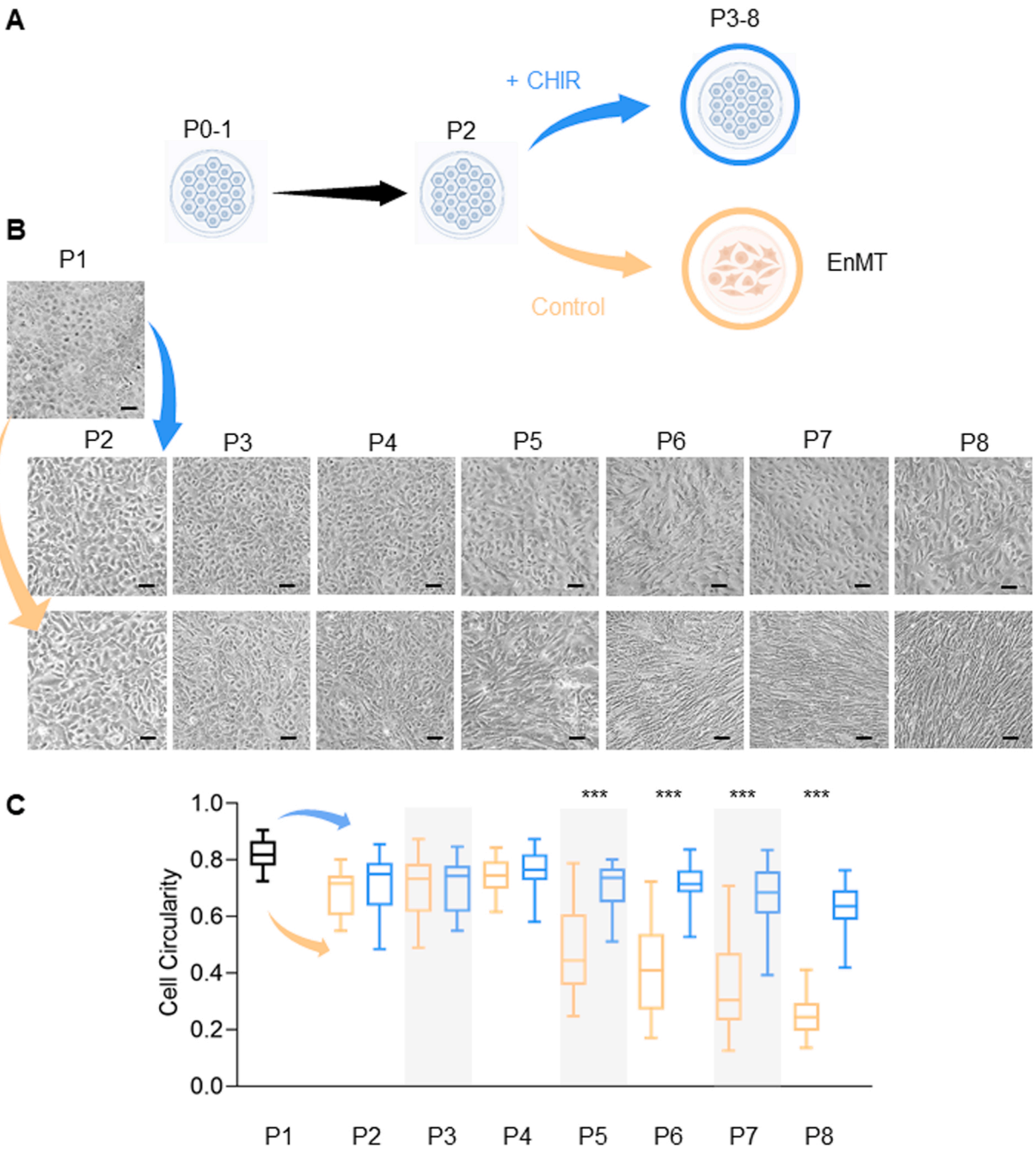

Fig. 4. CHIR preserves the polygonal phenotype in primary cultures of HCEnCs. A) Schematic representation of the experimental plan for CHIR addition to HCEnCs culture, before EnMT. Image created with Biorender.com B) Representative phase-contrast images of primary HCEnCs culture at progressive passages (P3 to P8) treated with CHIR before EnMT, showing the morphological differences with the untreated HCEnCs. Scale bar 100 μm. C) Box plot comparing cell circularity values between HCEnCs treated with CHIR and their relative untreated control (n = 3) at subsequent passages in culture. Cell circularity is expressed as values ± SD. Statistical significance was assessed using a Student t-test and set at $p < 0.05$. p values are indicated as following: ns (not significative) when $p > 0.05$, * when $p < 0.05$, * * when $p < 0.01$, * ** when $p < 0.001$.

expression of cell cycle inhibitors, that well matches the reduced proliferation (Fig. 5) as well as the reduced EnMT associated markers. Evaluation of other genes revealed possible new perspectives in the pathways that regulates HCEnCs growth and barrier formation.

3.7. *β-catenin signalling intersects with TGFβ pathway on HCEnCs*

Further analysis has been carried out on HCEnCs to better delineate the intracellular pathway regulation of β-catenin and TGFβ signalling upon CHIR and TGFβ Inhibitor (TGFβI) treatments (Fig. 7).

A morphological variation was assessed in HCEnCs at different passages: it was evident how CHIR preserved the hexagonal morphology, while the TGFβI and CHIR+TGFβI conditions did not show any improvement from the untreated control (Fig. 7 A shows representative images at P4). Quantification of cell circularity at P4 revealed a significant difference between CHIR treated and TGFβI or CHIR+TGFβI cells ($p < 0.0001$); while the latter two conditions did not appear different from the control (Fig. 7B).

Gene expression revealed that TGFβI treatment significantly decreases COL1A1 expression in HCEnCs ($p < 0.0001$), as known from

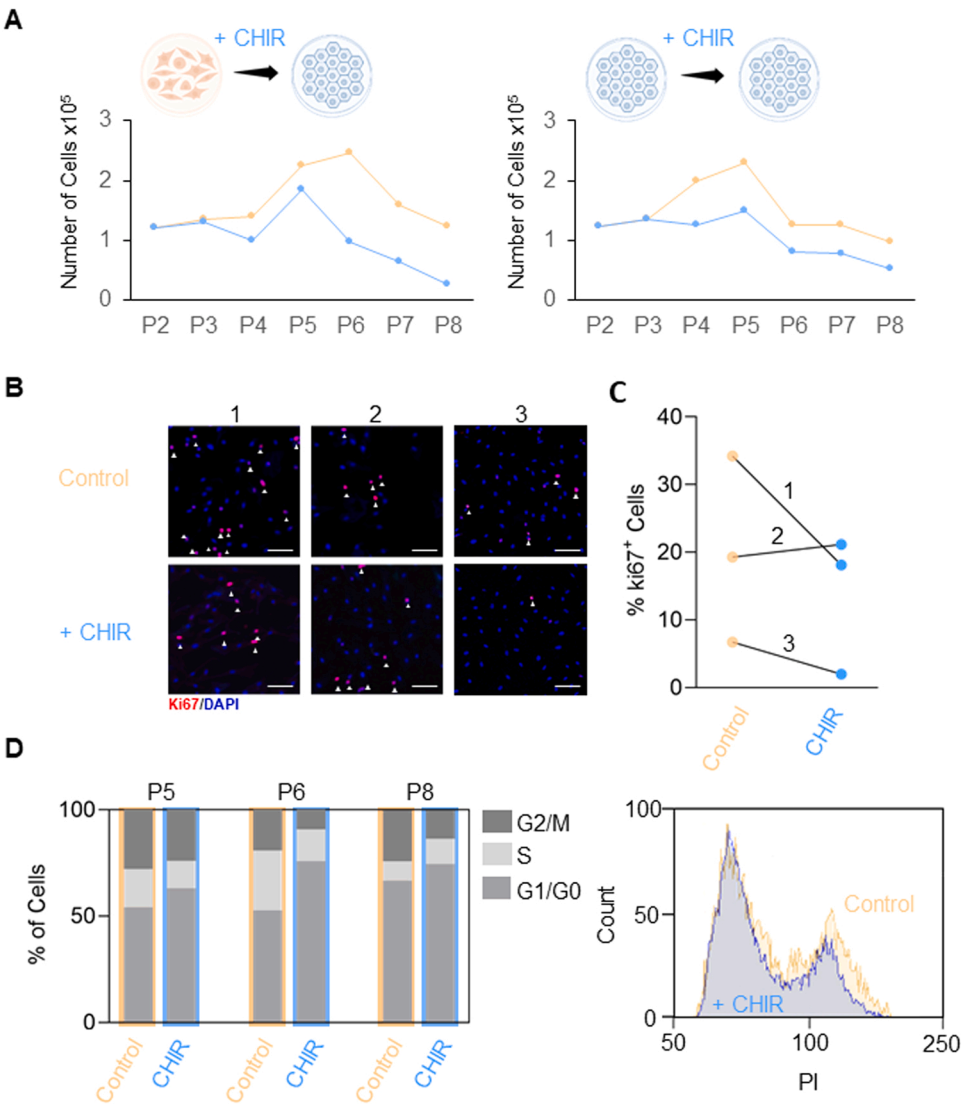

Fig. 5. CHIR reduces cell proliferation rate in primary cultures of HCEnCs. A) HCEnCs count (Number of cells x10^5) upon detachment at progressive passages, compared between CHIR treated and untreated HCEnCs. Graphs show representative values for HCEnCs where CHIR treatment started before and after EnMT. B) Immunofluorescence microscopy images showing expression of ki67 (red) marker in sub-confluent HCEnCs at P5, untreated or treated with CHIR. DAPI (blue) counterstains nuclei. Scale bar 100 μm. C) Quantification of the percentage of HCEnCs expressing ki67 protein as seen in Fig. 5B. D) Fluorescence Activated Cells Sorting (FACS) analysis of primary HCEnCs at P5-P6-P8 treated with CHIR and untreated control.

literature and similarly to what observed with the combined effect of CHIR+TGFβI ($p < 0.0001$). While inhibition of the TGFβ signalling did not result in a significant variation of α-SMA and CD44 expression, the cumulative effect of CHIR and TGFβI determined a significant down-regulation of the two EnMT markers ($p < 0.0001$).

The results obtained herein suggest that TGFβ and β-catenin act in a coordinated fashion to regulate HCEnCs expansion.

4. Discussion

The visual stimuli, fundamental for human quality of life, pass through a clear cornea. While the outer corneal epithelium is constantly renewed by stem cells (Pellegrini et al., 1997) and an advanced cell therapy is already a clinical practice (Pellegrini et al., 2016), regenerative medicine approaches are still at their debut for the inner CE (Kinoshita et al., 2018).

HCEnCs, although arrested in G1 phase of the cell cycle in vivo (Joyce et al., 1996), retain a low proliferative capacity in vitro that allows a limited expansion in culture. This is only possible for a short number of passages since HCEnCs easily undergo EnMT and lose the characteristic morphology and expression markers, required for their function (Frausto et al., 2020).

During EnMT, HCEnCs acquire an elongated shape and EnMT markers such as α-SMA (Zhu et al., 2012), while losing cell-cell contact and typical corneal endothelial markers such as ZO-1 and Na^+/K^+ ATPase (He et al., 2012). Several attempts have been made in preventing EnMT in HCEnCs culture through growth medium optimization (Bartakova et al., 2018; Peh et al., 2015) but no reports to date have thoroughly described a method for reverting the mesenchymal phenotype of HCEnCs for subsequent passages in culture, once they have undergone EnMT.

CHIR99021, a GSK-3β inhibitor that induces β-catenin activation, demonstrated capable of reverting the elongated shape in HCEnCs primary culture by reducing α-SMA expression and EnMT, while promoting the expression of characteristic CE markers and the formation of cell-cell junction upon confluency. Regulation of β-catenin was previously found to have a pivotal role in CEnCs expansion, since β-catenin related effectors were over-expressed in cells in vitro when compared with the corresponding corneal explants (Maurizi et al., 2020). This was partially explained by experiments proving how cellular proliferation of CEnCs was impaired by blocking β-catenin pathway (using quercetin). Although CHIR stimulation promoted β-catenin stability, it did not induce further proliferation (Maurizi et al., 2020). Nevertheless, the involvement of β-catenin pathway in other mechanisms of HCEnCs during cell expansion, such as EnMT (Zhu et al., 2012), has been proposed (Maurizi et al., 2020; Zhu et al., 2012), although it remains largely unexplored. The intracellular function of β-catenin is tissue and context specific and its interaction with different nuclear transcription factors

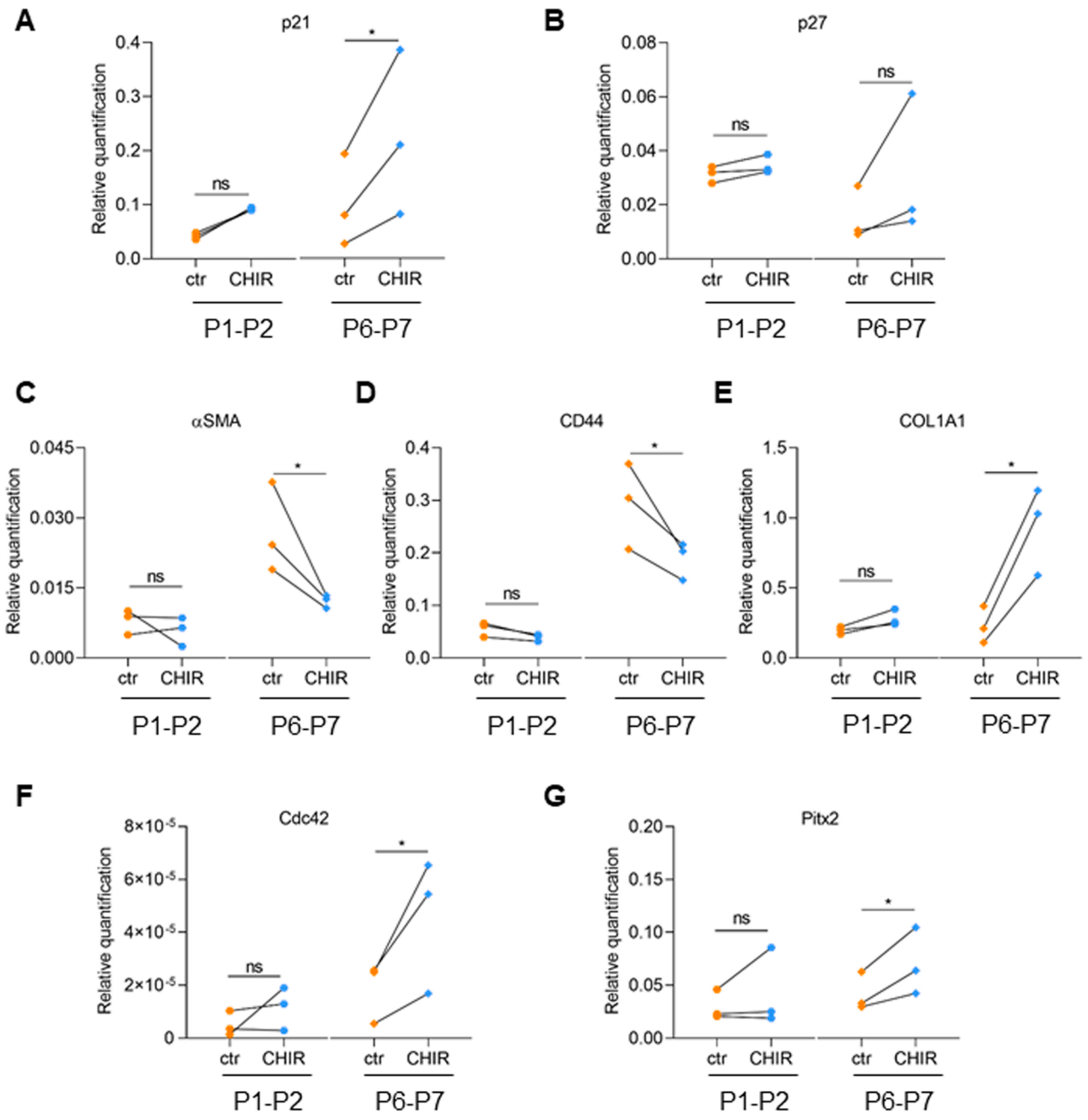

Fig. 6. CHIR effects on gene expression in primary cultures of HCEnCs. Panel of genes (p21, p27, α-SMA, CD44, COL1A1, CdC42, Pitx2) whose mRNA expression has been evaluated on primary HCEnCs at low (P1-P2) and high (P6-P7) passages by quantitative (q) RT-PCR. mRNA levels for each gene of the three donor derived HCEnCs cultures analysed are shown as relative expression. Statistical significance was assessed using a Student t-test (Ratio paired) and set at $p < 0.05$. p values are indicated as following: ns (not significative) when $p > 0.05$, * when $p < 0.05$, * * when $p < 0.01$, * ** when $p < 0.001$.

may promote alternative cellular processes (Chatterjee et al., 2015; Gao et al., 2021). Of particular interest, accumulating evidence indicates how this effector may push not only towards proliferation (Adachi et al., 2007; Dravid et al., 2005) but also toward differentiation (Huelsken et al., 2001; Ma et al., 2012; Otero et al., 2004). Moreover, β-catenin is also a key regulator of mesenchymal transformation during development (von Gise et al., 2011), fibrosis (Bowley et al., 2007; Ma et al., 2021) and wound healing (Stojadinovic et al., 2005). In accordance with this, we have demonstrated here that, when over-stimulated with 10 μM CHIR, β-catenin promotes EnMT; otherwise, when more finely tuned (1 μM CHIR), it blocks and reverts EnMT in primary HCEnCs for several subsequent passages in culture, also in old donors.

CHIR99021 has been selected as it represents a highly specific inhibitor of GSK-3 (Bennett et al., 2002; Li et al., 2009; Wang et al., 2022a; Ye et al., 2012).

The concentration range (1–10 μM) was chosen based on similar CHIR99021 ranges used in other works to determine its effects on primary human cells expression (Naujok et al., 2014) but also nuclear β-catenin induction (Chen et al., 2020; Huang et al., 2017; Wang et al., 2022b; Won et al., 2021).

CHIR99021 concentrations range of 1–10 μM, even if closely spaced, have a variable effect: 10 μM is cytotoxic in multiple cells if compared with the lower 5 μM (Neves et al., 2017) or 1 μM (Mussmann et al., 2007; Yoshida et al., 2018). CHIR99021 at low concentrations are generally well tolerated in corneal endothelial cells, being 3 μM (Wagoner et al., 2018; Zhao and Afshari, 2016) or 4 μM (Grönroos et al.,

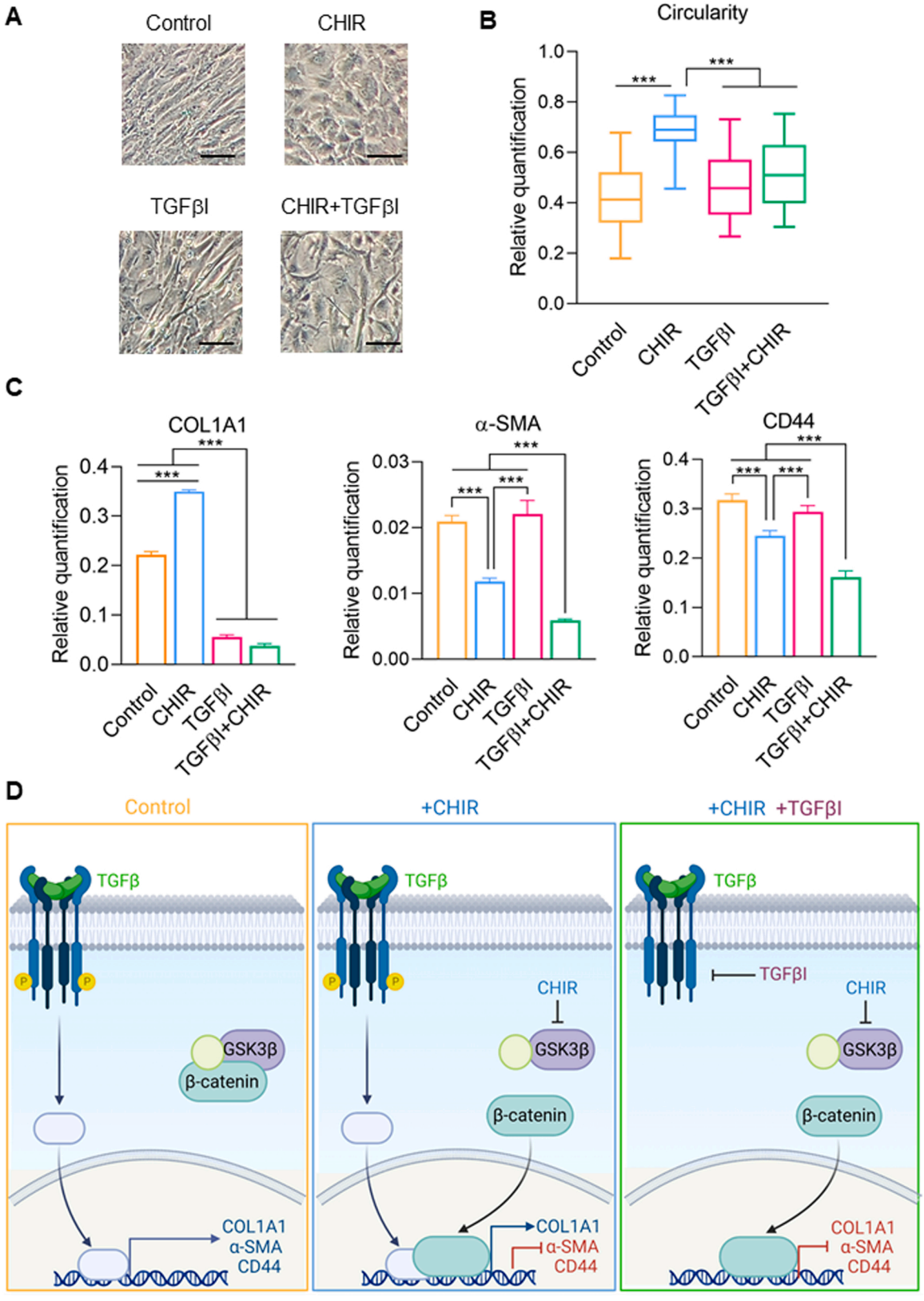

Fig. 7. β-catenin signalling intersects with TGFβ pathway on HCEnCs. A) Representative phase-contrast images of primary HCEnCs culture at P4 treated with CHIR, TGFβI and CHIR+TGFβI showing the morphological differences with the untreated HCEnCs. Scale bar 100 μm. B) Box plot comparing cell circularity values between HCEnCs treated and untreated cells at subsequent passages in culture. Cell circularity is expressed as values ± SD. C) mRNA expression of COL1A1, α-SMA and CD44 of primary HCEnCs culture at P4 (± SD). Statistical significance was assessed using a Student t-test (Ratio paired for the RT-PCR analysis) and set at $p < 0.05$. p values are indicated as following: ns (not significative) when $p > 0.05$, * when $p < 0.05$, * * when $p < 0.01$, * ** when $p < 0.001$. D) Schematic representation of a putative molecular pathway based on our finding, involving β-catenin and TGFβ. Image created with Biorender.com.

2021) previously chosen as a first step to differentiate human induced pluripotent stem cells to cells exhibiting characteristics of corneal endothelium.

Moreover, other GSK-3 inhibitors demonstrated a similar variable efficacy depending on their dose and cell specificity, including SB216763 that induces lymphatic endothelial cell proliferation at 1 μM but not at 10 μM (Stump et al., 2019). Another example is BIO that severely affects cell viability if used at 10 μM, while the same cell culture is not compromised if it is used at 1 μM (Mussmann et al., 2007).

In the present work, once CHIR was added to HCEnCs that had already underwent EnMT, cell morphology, as measured by cell circularity (Peh et al., 2015), was maintained through the passages up to passage 8, while α-SMA was significantly downregulated both at RNA and protein level and CD44, another marker of EnMT (Okumura et al., 2014), was significantly downregulated at RNA level. CEnCs markers such as Na^+/K^+ ATPase, N-cadherin and ZO-1 (He et al., 2021), were also preserved upon CHIR treatment. The same result was obtained by adding CHIR in HCEnCs that still maintained a normal hexagonal phenotype. In accordance with the observed ability of promoting barrier formation while reverting the EnMT process, β-catenin retains a role in stabilizing the tight junctions by increasing ZO-1 expression (Ji et al., 2021).

All together, these results suggest how EnMT may be reversed, at least until a certain limit. Consistently with this observation, sub-confluent HCEnCs culture presented a slight elongated phenotype, both in control and CHIR treated cells, independently from the phenotype they reacquired when confluent, either hexagonal or elongated. These data suggest that HCEnCs may undergo a transient mesenchymal transformation when proliferating and a subsequent mesenchymal-to-endothelial (MEnT) transformation when reaching confluency. Although some observations reported here are only hints of this process, this aspect should be further confirmed and investigated to identify possible key regulators orchestrating this reversible mechanism.

As we previously noticed (Maurizi et al., 2020), treatment with CHIR did not stimulate proliferation nor induced cell death; on the contrary it slightly decreased cells entering G2/M and consequently actively proliferating, probably through the activation of cell cycle inhibitors p21 and p27 that we found significantly overexpressed in CHIR treated cells. This result is in contrast with what reported by Wang et al. in a corneal endothelial cell line (B4G12), where CHIR stimulation promoted an increased proliferation (Wang et al., 2022b). However, the B4G12 cell line is not comparable to a human corneal endothelial primary culture as presenting a different pattern of marker expression, and an altered cellular proliferation mechanism is typical in immortalised cell lines (Frausto and Aldave, 2014; Ha Thi et al., 2014).

Furthermore, here we found how the intersection of β-catenin pathway with that of TGF-β regulates Collagen I expression. Although also described as a marker of EnMT (Lee et al., 2012), Collagen I is involved in tissue wound healing, a process that requires extracellular matrix deposition and remodelling (Mathew-Steiner et al., 2021). TGF-β is a well known regulator of Collagen I expression (Rossert et al., 2000) and here we confirmed that, by inhibiting this pathway, Collagen I expression was severely down-regulated. Conversely, CHIR stimulation promoted an increase of Collagen I expression, possibly because the interaction of both (TGFβ and β-catenin) pathways is necessary to stimulate Collagen I production. On the other hand, inhibition of TGFβ did not decrease α-SMA and CD44 expression, nor reverted cellular morphology toward a hexagonal shape, while CHIR stimulation was able to promote the latter processes associated with EnMT. A combination of CHIR and TGFβI induced in part a cumulative effect: it reduced Collagen I expression and further decreased expression of α-SMA and CD44. However, there was not any improvement on the cellular shape if compared with the CHIR condition, suggesting that the intersection of TGFβ and β-catenin is important in HCEnCs for maintenance of the correct morphology.

The cumulative downregulation of α-SMA and CD44 might be caused by a sustained regulatory effect of TGFβ downstream effectors (Smad) on β-catenin function. Intriguingly, this combined effect is in contrast with reports on other cellular types (Zhou et al., 2012), confirming the context specificity of the β-catenin regulated processes. Altogether, these results support the hypothesis of a crosstalk between TGFβ and β-catenin pathways that is responsible for CEnCs fate, although the combined effect caused by a concomitant dysregulation should be further dissected, considering different dosages and timings. To define whether up-regulation of the β-catenin pathway may have an impact on indirect pathways also we analysed the expression of other effectors, selected based on previous findings in CE.

Although not highly expressed in HCEnCs, Cdc42, a downstream target of the non-canonical Wnt pathway resulted significantly upregulated at high passages following CHIR treatment, as previously observed in B4G12 cell line (Wang et al., 2022b). However, while in B4G12 it was associated to an increased proliferation, herein it correlates with a decreased cell growth, similarly to what previously found in neural stem cells (Chavali et al., 2018).

Pitx2, a homeobox gene involved in corneal development through Wnt interaction (Gage et al., 2014), was found here upregulated upon β-catenin stabilization, as previously observed in HCEnCs by (Hatou et al., 2013), revealing a possible role for this gene in supporting β-catenin for determining cell fate.

Collectively, this work identified CHIR99021 as a single factor able to revert the elongeted phenotype of HCEnCs for several subsequent passages in culture. When considering different donors, the extent of CHIR99021 effect was different even though we could always detect an improvement in cell morphology towards a polygonal shape in any culture treated with CHIR99021 at 1 μM, if compared to the control. The difference between donors could be appreciated also when comparing gene expression analysis from different donors (Fig. 7). CHIR99021, through specific GSK-3β inhibition and the consequent cytoplasmic β-catenin stabilization, promotes corneal endothelial differentiation from an elongated to a hexagonal phenotype. HCEnCs pass through a transient EnMT during expansion in culture (sub-confluence) that is reverted at confluency only if β-catenin is properly dosed, in order to induce the correct phenotype and junction formation. Thus, based on the findings of this study, CHIR99021 inhibits EnMT in corneal endothelium through β-catenin stabilization, which interacts with other pathways such as TGFβ for determining cell differentiation.

5. Conclusions

The identification of CHIR as a single factor able to revert the HCEnCs elongated phenotype in culture represents a substantial achievement for maintaining HCEnCs morphology and markers in vitro until late passages.

Further investigations are necessary for unravelling the precise mechanisms involved in HCEnCs proliferation and differentiation, and how Wnt/β-catenin pathway interplays with others, such as TGFβ's. These findings would lay the path for developing therapeutic strategies in vitro under Good Manufacturing Practice (GMP) conditions (De Rosa et al., 2021) or in vivo using compounds that maintain corneal endothelial differentiation, such as CHIR, alone or in combination with other factors that promote a controlled cell proliferation.

Funding

This research did not receive any specific grant from funding agencies in the public, commercial, or not-for-profit sectors. This research was supported by the prestigious international Louis Jeantet-Collen prize for Translational Medicine and by the prize Lombardia è ricerca, won by Prof. Graziella Pellegrini and Prof. Michele De Luca (University of Modena and Reggio Emilia, Italy). Additional funding was provided by Prof. Claudio Macaluso (University of Parma, Italy).

Ethical statement

Donor human corneas from Italian Eye Banks, unsuitable for transplantation, were obtained with their relatives written consent for research use. The tissues were handled in accordance with the declaration of Helsinki. The experimental protocol was approved by ISS-CNT (Italian National Transplant Centre) and by the local ethical committee (Comitato Etico dell'Area Vasta Emilia Nord, p. 0002956/20).

CRediT authorship contribution statement

E.M., A.M., D.S. and G.P.: Conceptualization and design. E.M., A.M.: data collection. E.M., D.S., A.M. and G.P.: data analysis and interpretation. C.M. and G.P.: Funding acquisition. E.M., D.S.: manuscript Writing – original draft. E.M., A.M., C.M., D.S. and G.P.: manuscript editing and final approval.

Declaration of Competing Interest

The authors declare the following financial interests/personal relationships which may be considered as potential competing interests: Prof. Graziella Pellegrini is in the board of directors of Holostem Terapie Avanzate S.r.l. Holostem Terapie Avanzate S.r.l. owns a patent (n. 102022000020061) filed the 29th of September 2022.

Acknowledgments

The authors would like to thank the researchers and the students that helped within this project. A special thank must go to the people who donated their organs for medical or research purposes.

Appendix A. Supporting information

Supplementary data associated with this article can be found in the online version at doi:10.1016/j.ejcb.2023.151302.

References

Adachi, K., Mirzadeh, Z., Sakaguchi, M., Yamashita, T., Nikolcheva, T., Gotoh, Y., Peltz, G., Gong, L., Kawase, T., Alvarez-Buylla, A., 2007. β-Catenin signaling promotes proliferation of progenitor cells in the adult mouse subventricular zone. Stem Cells 25, 2827–2836.

Ali, M., Raghunathan, V., Li, J.Y., Murphy, C.J., Thomasy, S.M., 2016. Biomechanical relationships between the corneal endothelium and Descemet's membrane. Exp. eye Res. 152, 57–70.

Bartakova, A., Kuzmenko, O., Alvarez-Delfin, K., Kunzevitzky, N.J., Goldberg, J.L., 2018. A cell culture approach to optimized human corneal endothelial cell function. Invest. Ophthalmol. Vis. Sci. 59, 1617–1629.

Bennett, C.N., Ross, S.E., Longo, K.A., Bajnok, L., Hemati, N., Johnson, K.W., Harrison, S. D., MacDougald, O.A., 2002. Regulation of Wnt signaling during adipogenesis. J. Biol. Chem. 277, 30998–31004.

Bourne, W., 2003. Biology of the corneal endothelium in health and disease. Eye 17, 912–918.

Bowley, E., O'Gorman, D.B., Gan, B.S., 2007. β-catenin signaling in fibroproliferative disease. J. Surg. Res. 138, 141–150.

Català, P., Thuret, G., Skottman, H., Mehta, J.S., Parekh, M., Dhubhghaill, S.N., Collin, R. W., Nuijts, R.M., Ferrari, S., LaPointe, V.L., 2021. Approaches for corneal endothelium regenerative medicine. Prog. Retin. eye Res., 100987

Chang, Y.K., Hwang, J.S., Chung, T.-Y., Shin, Y.J., 2018. SOX2 activation using CRISPR/dCas9 promotes wound healing in corneal endothelial cells. Stem Cells 36, 1851–1862.

Chatterjee, S.S., Saj, A., Gocha, T., Murphy, M., Gonsalves, F.C., Zhang, X., Hayward, P., Akgöl Oksuz, B., Shen, S.S., Madar, A., 2015. Inhibition of β-catenin–TCF1 interaction delays differentiation of mouse embryonic stem cells. J. Cell Biol. 211, 39–51.

Chavali, M., Klingener, M., Kokkosis, A.G., Garkun, Y., Felong, S., Maffei, A., Aguirre, A., 2018. Non-canonical Wnt signaling regulates neural stem cell quiescence during homeostasis and after demyelination. Nat. Commun. 9, 1–17.

Chen, J., Yang, Y., Li, S., Yang, Y., Dai, Z., Wang, F., Wu, Z., Tso, P., Wu, G., 2020. E2F1 regulates adipocyte differentiation and adipogenesis by activating ICAT. Cells 9, 1024.

De Rosa, L., Enzo, E., Zardi, G., Bodemer, C., Magnoni, C., Schneider, H., De Luca, M., 2021. Hologene 5: A Phase II/III Clinical Trial of Combined Cell and Gene Therapy of Junctional Epidermolysis Bullosa. Front Genet 12, 705019. https://doi.org/10.3389/fgene.2021.705019.

Distler, J.H., Györfi, A.-H., Ramanujam, M., Whitfield, M.L., Königshoff, M., Lafyatis, R., 2019. Shared and distinct mechanisms of fibrosis. Nat. Rev. Rheumatol. 15, 705–730.

Dravid, G., Ye, Z., Hammond, H., Chen, G., Pyle, A., Donovan, P., Yu, X., Cheng, L., 2005. Defining the role of Wnt/β-catenin signaling in the survival, proliferation, and self-renewal of human embryonic stem cells. Stem Cells 23, 1489–1501.

Frausto, R.F., Aldave, A.J., 2014. Comparing the transcriptome of ex vivo endothelium with cultured human corneal endothelial cells. Invest. Ophthalmol. Vis. Sci. 55, 3585-3585.

Frausto, R.F., Swamy, V.S., Peh, G.S., Boere, P.M., Hanser, E.M., Chung, D., George, B.L., Morselli, M., Kao, L., Azimov, R., 2020. Phenotypic and functional characterization of corneal endothelial cells during in vitro expansion. Sci. Rep. 10, 1–22.

Gage, P.J., Kuang, C., Zacharias, A.L., 2014. The homeodomain transcription factor PITX2 is required for specifying correct cell fates and establishing angiogenic privilege in the developing cornea. Dev. Dyn.: Off. Publ. Am. Assoc. Anat. 243, 1391–1400. https://doi.org/10.1002/dvdy.24165.

Gao, J., Liao, Y., Qiu, M., Shen, W., 2021. Wnt/β-catenin signaling in neural stem cell homeostasis and neurological diseases. Neuroscientist 27, 58–72.

von Gise, A., Zhou, B., Honor, L.B., Ma, Q., Petryk, A., Pu, W.T., 2011. WT1 regulates epicardial epithelial to mesenchymal transition through β-catenin and retinoic acid signaling pathways. Dev. Biol. 356, 421–431.

Grönroos, P., Ilmarinen, T., Skottman, H., 2021. Directed differentiation of human pluripotent stem cells towards corneal endothelial-like cells under defined conditions. Cells 10, 331.

Gu, X., Seong, G.J., Lee, Y.G., Kay, E., 1996. Fibroblast growth factor 2 uses distinct signaling pathways for cell proliferation and cell shape changes in corneal endothelial cells. Invest. Ophthalmol. Vis. Sci. 37, 2326–2334.

Ha Thi, B.M., Campolmi, N., He, Z., Pipparelli, A., Manissolle, C., Thuret, J.-Y., Piselli, S., Forest, F., Peoc'h, M., Garraud, O., 2014. Microarray analysis of cell cycle gene expression in adult human corneal endothelial cells. PLoS One 9, e94349.

Hatou, S., Yoshida, S., Higa, K., Miyashita, H., Inagaki, E., Okano, H., Tsubota, K., Shimmura, S., 2013. Functional corneal endothelium derived from corneal stroma stem cells of neural crest origin by retinoic acid and Wnt/β-catenin signaling. Stem Cells Dev. 22, 828–839.

He, Z., Campolmi, N., Gain, P., Ha Thi, B.M., Dumollard, J.-M., Duband, S., Peoc'h, M., Piselli, S., Garraud, O., Thuret, G., 2012. Revisited microanatomy of the corneal endothelial periphery: new evidence for continuous centripetal migration of endothelial cells in humans. Stem Cells 30, 2523–2534.

He, Z., Okumura, N., Sato, M., Komori, Y., Nakahara, M., Gain, P., Koizumi, N., Thuret, G., 2021. Corneal endothelial cell therapy: feasibility of cell culture from corneas stored in organ culture. Cell Tissue Bank. 22, 551–562.

Hirata-Tominaga, K., Nakamura, T., Okumura, N., Kawasaki, S., Kay, E.P., Barrandon, Y., Koizumi, N., Kinoshita, S., 2013. Corneal endothelial cell fate is maintained by LGR5 through the regulation of hedgehog and Wnt pathway. Stem Cells 31, 1396–1407.

Huang, J., Guo, X., Li, W., Zhang, H., 2017. Activation of Wnt/β-catenin signalling via GSK3 inhibitors direct differentiation of human adipose stem cells into functional hepatocytes. Sci. Rep. 7, 1–12.

Huelsken, J., Vogel, R., Erdmann, B., Cotsarelis, G., Birchmeier, W., 2001. β-Catenin controls hair follicle morphogenesis and stem cell differentiation in the skin. Cell 105, 533–545.

Ji, Y.-B., Gao, Q., Tan, X.-X., Huang, X.-W., Ma, Y.-Z., Fang, C., Wang, S.-N., Qiu, L.-H., Cheng, Y.-X., Guo, F.-Y., 2021. Lithium alleviates blood-brain barrier breakdown after cerebral ischemia and reperfusion by upregulating endothelial Wnt/β-catenin signaling in mice. Neuropharmacology 186, 108474.

Joyce, N.C., 2004. Human corneal endothelial cell proliferation: potential for use in regenerative medicine. Cornea 23, S8–S19.

Joyce, N.C., 2005. Cell cycle status in human corneal endothelium. Exp. eye Res. 81, 629–638.

Joyce, N.C., Navon, S.E., Roy, S., Zieske, J.D., 1996. Expression of cell cycle-associated proteins in human and rabbit corneal endothelium in situ. Invest. Ophthalmol. Vis. Sci. 37, 1566–1575.

Kinoshita, S., Koizumi, N., Ueno, M., Okumura, N., Imai, K., Tanaka, H., Yamamoto, Y., Nakamura, T., Inatomi, T., Bush, J., 2018. Injection of cultured cells with a ROCK inhibitor for bullous keratopathy. N. Engl. J. Med. 378, 995–1003.

Laco, F., Woo, T.L., Zhong, Q., Szmyd, R., Ting, S., Khan, F.J., Chai, C.L., Reuveny, S., Chen, A., Oh, S., 2018. Unraveling the inconsistencies of cardiac differentiation efficiency induced by the GSK3β inhibitor CHIR99021 in human pluripotent stem cells. Stem Cell Rep. 10, 1851–1866.

Lam, A.Q., Freedman, B.S., Morizane, R., Lerou, P.H., Valerius, M.T., Bonventre, J.V., 2014. Rapid and efficient differentiation of human pluripotent stem cells into intermediate mesoderm that forms tubules expressing kidney proximal tubular markers. J. Am. Soc. Nephrol. 25, 1211–1225.

Lambert, A.W., Weinberg, R.A., 2021. Linking EMT programmes to normal and neoplastic epithelial stem cells. Nat. Rev. Cancer 21, 325–338.

Leach, L.L., Buchholz, D.E., Nadar, V.P., Lowenstein, S.E., Clegg, D.O., 2015. Canonical/β-catenin Wnt pathway activation improves retinal pigmented epithelium derivation from human embryonic stem cells. Invest. Ophthalmol. Vis. Sci. 56, 1002–1013.

Leclerc, V.B., Roy, O., Santerre, K., Proulx, S., 2018. TGF-β1 promotes cell barrier function upon maturation of corneal endothelial cells. Sci. Rep. 8, 4438.

Lee, J., Jung, E., Gestoso, K., Heur, M., 2020. ZEB1 Mediates fibrosis in corneal endothelial mesenchymal transition through SP1 and SP3. Invest Ophthalmol. Vis. Sci. 61 (41) https://doi.org/10.1167/iovs.61.8.41.

Lee, J.G., Heur, M., 2015. WNT10B enhances proliferation through β-catenin and RAC1 GTPase in human corneal endothelial cells. J. Biol. Chem. 290, 26752–26764.

Lee, J.G., Kay, E.P., 2008. Involvement of two distinct ubiquitin E3 ligase systems for p27 degradation in corneal endothelial cells. Invest. Ophthalmol. Vis. Sci. 49, 189–196.
Lee, J.G., Ko, M.K., Kay, E.P., 2012. Endothelial mesenchymal transformation mediated by IL-1β-induced FGF-2 in corneal endothelial cells. Exp. eye Res. 95, 35–39.
Lee, J.G., Jung, E., Heur, M., 2018. Fibroblast growth factor 2 induces proliferation and fibrosis via SNAI1-mediated activation of CDK2 and ZEB1 in corneal endothelium. J. Biol. Chem. 293, 3758–3769.
Li, W., Sabater, A.L., Chen, Y.-T., Hayashida, Y., Chen, S.-Y., He, H., Tseng, S.C., 2007. A novel method of isolation, preservation, and expansion of human corneal endothelial cells. Invest. Ophthalmol. Vis. Sci. 48, 614–620.
Li, W., Zhou, H., Abujarour, R., Zhu, S., Young Joo, J., Lin, T., Hao, E., Schöler, H.R., Hayek, A., Ding, S., 2009. Generation of human-induced pluripotent stem cells in the absence of exogenous Sox2. Stem Cells 27, 2992–3000.
Ma, J., Wang, R., Fang, X., Sun, Z., 2012. β-catenin/TCF-1 pathway in T cell development and differentiation. J. Neuroimmune Pharm. 7, 750–762.
Ma, X., Long, C., Wang, F., Lou, B., Yuan, M., Duan, F., Yang, Y., Li, J., Qian, X., Zeng, J., 2021. METTL3 attenuates proliferative vitreoretinopathy and epithelial-mesenchymal transition of retinal pigment epithelial cells via wnt/β-catenin pathway. J. Cell. Mol. Med 25, 4220–4234.
Mathew-Steiner, S.S., Roy, S., Sen, C.K., 2021. Collagen in wound healing. Bioeng. (Basel, Switz.) 8. https://doi.org/10.3390/bioengineering8050063.
Maurizi, E., Schiroli, D., Zini, R., Limongelli, A., Mistò, R., Macaluso, C., Pellegrini, G., 2020. A fine-tuned β-catenin regulation during proliferation of corneal endothelial cells revealed using proteomics analysis. Sci. Rep. 10, 1–16.
Maurizi, E., Martella, D.A., Schiroli, D., Merra, A., Mustfa, S.A., Pellegrini, G., Macaluso, C., Chiappini, C., 2022a. Nanoneedles Induce Target. siRNA Silenci p16 Hum. Corneal Endothel. 9, e2203257 https://doi.org/10.1002/advs.202203257.
Maurizi, E., Merra, A., Schiroli, D., Ghezzi, B., Macaluso, C., Pellegrini, G., 2022b. Fluctuations in corneal endothelial LAP2 expression levels correlate with passage dependent declines in their cell proliferative activity. Int. J. Mol. Sci. 23, 5859.
Mussmann, R., Geese, M., Harder, F., Kegel, S., Andag, U., Lomow, A., Burk, U., Onichtchouk, D., Dohrmann, C., Austen, M., 2007. Inhibition of GSK3 promotes replication and survival of pancreatic beta cells. J. Biol. Chem. 282, 12030–12037.
Naujok, O., Diekmann, U., Lenzen, S., 2014. The generation of definitive endoderm from human embryonic stem cells is initially independent from activin A but requires canonical Wnt-signaling. Stem Cell Rev. Rep. 10, 480–493.
Neves, V., Babb, R., Chandrasekaran, D., Sharpe, P.T., 2017. Promotion of natural tooth repair by small molecule GSK3 antagonists. Sci. Rep. 7, 1–7.
Nusse, R., Fuerer, C., Ching, W., Harnish, K., Logan, C., Zeng, A., Ten Berge, D., Kalani, Y., Year Wnt signaling and stem cell control. In Cold Spring Harb. Symp. Quant. Biol.
Okumura, N., Koizumi, N., Ueno, M., Sakamoto, Y., Takahashi, H., Tsuchiya, H., Hamuro, J., Kinoshita, S., 2012. ROCK inhibitor converts corneal endothelial cells into a phenotype capable of regenerating in vivo endothelial tissue. Am. J. Pathol. 181, 268–277.
Okumura, N., Kay, E.P., Nakahara, M., Hamuro, J., Kinoshita, S., Koizumi, N., 2013. Inhibition of TGF-β signaling enables human corneal endothelial cell expansion in vitro for use in regenerative medicine. PLoS One 8, e58000.
Okumura, N., Hirano, H., Numata, R., Nakahara, M., Ueno, M., Hamuro, J., Kinoshita, S., Koizumi, N., 2014. Cell surface markers of functional phenotypic corneal endothelial cells. Invest. Ophthalmol. Vis. Sci. 55, 7610–7618.
Okumura, N., Kakutani, K., Numata, R., Nakahara, M., Schlötzer-Schrehardt, U., Kruse, F., Kinoshita, S., Koizumi, N., 2015. Laminin-511 and-521 enable efficient in vitro expansion of human corneal endothelial cells. Invest. Ophthalmol. Vis. Sci. 56, 2933–2942.
Otero, J.J., Fu, W., Kan, L., Cuadra, A.E., Kessler, J.A., 2004. β-Catenin signaling is required for neural differentiation of embryonic stem cells.
Parekh, M., Ahmad, S., Ruzza, A., Ferrari, S., 2017. Human corneal endothelial cell cultivation from old donor corneas with forced attachment. Sci. Rep. 7, 1–12.
Parekh, M., Peh, G., Mehta, J.S., Ramos, T., Ponzin, D., Ahmad, S., Ferrari, S., 2019. Passaging capability of human corneal endothelial cells derived from old donors with and without accelerating cell attachment. Exp. Eye Res. 189, 107814.
Parekh, M., Ramos, T., O'Sullivan, F., Meleady, P., Ferrari, S., Ponzin, D., Ahmad, S., 2021. Human corneal endothelial cells from older donors can be cultured and passaged on cell-derived extracellular matrix. Acta Ophthalmol. (Copenh.) 99, e512–e522.
Paull, A.C., Whikehart, D.R., 2005. Expression of the p53 family of proteins in central and peripheral human corneal endothelial cells. Mol. Vis. 11, 328–334.
Peh, G.S., Toh, K.-P., Wu, F.-Y., Tan, D.T., Mehta, J.S., 2011. Cultivation of human corneal endothelial cells isolated from paired donor corneas. PLoS One 6, e28310.
Peh, G.S., Chng, Z., Ang, H.-P., Cheng, T.Y., Adnan, K., Seah, X.-Y., George, B.L., Toh, K.-P., Tan, D.T., Yam, G.H., 2015. Propagation of human corneal endothelial cells: a novel dual media approach. Cell Transplant. 24, 287–304.
Pellegrini, G., Traverso, C.E., Franzi, A.T., Zingirian, M., Cancedda, R., De Luca, M., 1997. Long-term restoration of damaged corneal surfaces with autologous cultivated corneal epithelium. Lancet 349, 990–993.
Pellegrini, G., Lambiase, A., Macaluso, C., Pocobelli, A., Deng, S., Cavallini, G.M., Esteki, R., Rama, P., 2016. From discovery to approval of an advanced therapy medicinal product-containing stem cells, in the EU. Regen. Med. 11, 407–420.
Rossert, J., Terraz, C., Dupont, S., 2000. Regulation of type I collagen genes expression. Nephrol. Dial. Transplant. 15, 66–68.
Roy, O., Leclerc, V.B., Bourget, J.-M., Thériault, M., Proulx, S., 2015. Understanding the process of corneal endothelial morphological change in vitro. Invest. Ophthalmol. Vis. Sci. 56, 1228–1237.
Stojadinovic, O., Brem, H., Vouthounis, C., Lee, B., Fallon, J., Stallcup, M., Merchant, A., Galiano, R.D., Tomic-Canic, M., 2005. Molecular pathogenesis of chronic wounds: the role of β-catenin and c-myc in the inhibition of epithelialization and wound healing. Am. J. Pathol. 167, 59–69.
Stump, B., Shrestha, S., Lamattina, A.M., Louis, P.H., Cho, W., Perrella, M.A., Ai, X., Rosas, I.O., Wagner, F.F., Priolo, C., 2019. Glycogen synthase kinase 3-β inhibition induces lymphangiogenesis through β-catenin-dependent and mTOR-independent pathways. PloS One 14, e0213831.
Van den Bogerd, B., Dhubhghaill, S.N., Koppen, C., Tassignon, M.-J., Zakaria, N., 2018. A review of the evidence for in vivo corneal endothelial regeneration. Surv. Ophthalmol. 63, 149–165.
Wagoner, M.D., Bohrer, L.R., Aldrich, B.T., Greiner, M.A., Mullins, R.F., Worthington, K. S., Tucker, B.A., Wiley, L.A., 2018. Feeder-free differentiation of cells exhibiting characteristics of corneal endothelium from human induced pluripotent stem cells. Biol. Open 7 bio032102.
Wang, B., Khan, S., Wang, P., Wang, X., Liu, Y., Chen, J., Tu, X., 2022a. A highly selective GSK-3β inhibitor CHIR99021 promotes osteogenesis by activating canonical and autophagy-mediated Wnt signaling. Front. Endocrinol. 13, 926622.
Wang, Y., Jin, C., Tian, H., Xu, J., Chen, J., Hu, S., Li, Q., Lu, L., Ou, Q., Xu, G.-t, 2022b. CHIR99021 balance TGFβ1 induced human corneal endothelial-to-mesenchymal transition to favor corneal endothelial cell proliferation. Exp. eye Res. 219, 108939.
Waring III, G.O., Bourne, W.M., Edelhauser, H.F., Kenyon, K.R., 1982. The corneal endothelium: normal and pathologic structure and function. Ophthalmology 89, 531–590.
Won, D.-H., Hwang, D.-B., Shin, Y.-S., Kim, S.-Y., Kim, C., Hong, I.-S., Kang, B.-C., Che, J.-H., Yun, J.-W., 2021. Cellular signaling crosstalk between Wnt signaling and gap junctions inbenzo [a] pyrene toxicity. Cell Biol. Toxicol. 1–18.
Wörner, C.H., Olguín, A., Ruíz-García, J.L., Garzón-Jiménez, N., 2011. Cell pattern in adult human corneal endothelium. PLoS One 6, e19483. https://doi.org/10.1371/journal.pone.0019483.
Ye, S., Tan, L., Yang, R., Fang, B., Qu, S., Schulze, E.N., Song, H., Ying, Q., Li, P., 2012. Pleiotropy of glycogen synthase kinase-3 inhibition by CHIR99021 promotes self-renewal of embryonic stem cells from refractory mouse strains. PloS One 7, e35892.
Yoshida, T., Sopko, N.A., Kates, M., Liu, X., Joice, G., McConkey, D.J., Bivalacqua, T.J., 2018. Three-dimensional organoid culture reveals involvement of Wnt/β-catenin pathway in proliferation of bladder cancer cells. Oncotarget 9, 11060.
Zhang, J., Tian, X.-J., Xing, J., 2016. Signal transduction pathways of EMT induced by TGF-β, SHH, and WNT and their crosstalks. J. Clin. Med. 5, 41.
Zhao, J.J., Afshari, N.A., 2016. Generation of human corneal endothelial cells via in vitro ocular lineage restriction of pluripotent stem cells. Invest. Ophthalmol. Vis. Sci. 57, 6878–6884.
Zhou, B., Liu, Y., Kahn, M., Ann, D.K., Han, A., Wang, H., Nguyen, C., Flodby, P., Zhong, Q., Krishnaveni, M.S., 2012. Interactions between β-catenin and transforming growth factor-β signaling pathways mediate epithelial-mesenchymal transition and are dependent on the transcriptional co-activator cAMP-response element-binding protein (CREB)-binding protein (CBP). J. Biol. Chem. 287, 7026–7038.
Zhu, Y.-T., Chen, H.-C., Chen, S.-Y., Tseng, S.C., 2012. Nuclear p120 catenin unlocks mitotic block of contact-inhibited human corneal endothelial monolayers without disrupting adherent junctions. J. Cell Sci. 125, 3636–3648.